Visualization of Neural Cell Adhesion Molecule by Electron Microscopy

Alison K. Hall*‡ and Urs Rutishauser*

*Neurobiology Program, Department of Developmental Genetics and Anatomy, Case Western Reserve University, School of Medicine, Cleveland, Ohio 44106; and ‡Laboratory of Neurobiology, National Institute of Neurological and Communicative Disorders and Stroke, National Institutes of Health, Department of Health and Human Services at the Marine Biological Laboratory, Woods Hole, MA 02543

Abstract. The 130- and 160-kD polypeptide forms of the neural cell adhesion molecule (NCAM) were analyzed by electron microscopy after low angle rotary shadowing and freeze replication. Individual NCAM molecules appeared as uniformly thick rods, with a distinct bend or hinge region near their middle. Aggregates were also present, containing two to six rods in a pinwheel-like configuration without measurable overlap between rods. The 130- and 160-kD NCAM forms had lengths of 38 and 51 nm, respectively, with a difference in arm length distal to the bend, but not toward the center of the pinwheel. Although enzymatic removal of the polysialic acid moiety on NCAM did not alter the appearance of individual molecules, it did increase the average number of arms per aggregate. Monoclonal antibodies that recognize defined regions of the NCAM polypeptide were used to provide landmarks on the observed molecular figures. Two antibodies specific for cytoplasmic epitopes near the COOH terminus were clustered at the distal tip of aggregated arms. Two other antibodies that react with epitopes near the NH_2 terminus and the middle of the molecule bound to sites more centrally located on the pinwheel structure. Together, these results suggest that the observed aggregates represent an association of molecules near their NH_2-terminal homophilic binding site, and have led to several predictions about the nature of an NCAM-mediated cell–cell bond.

THE neural cell adhesion molecule (NCAM) is a transmembranous sialoglycoprotein that serves as a ligand in cell–cell adhesion. NCAM-mediated adhesion is believed to play a role in a variety of developmental events involving several cell types, including neurons, muscle, and glial cells (for review see references 5 and 21). Though derived from a single gene, NCAM has a variety of structural variants, including differences in sialic acid content which appear to modulate the molecule's binding activity, and has at least three polypeptide forms with deglycosylated M_rs of 160, 130, and 110 kD (see reference 22). These NCAM proteins appear to be similar in their extracellular protein domains, including the putative cell–cell binding region (23, 4) and a common NH_2-terminal amino acid sequence (20) and differ primarily in the length of the cytoplasmic extension (9, 12). The 160-kD polypeptide has the longest intracellular domain, comprised of ~52 kD (12), while the 130-kD form has a shorter intracellular extension, and the 110-kD form may not completely penetrate the membrane (9).

To obtain a more complete description of structure–function relationships for NCAM, we have taken two complimentary approaches: (*a*) the characterization and linear mapping of monoclonal antibody epitopes (30, 8) and (*b*) the examination of the molecule's shape and aggregation properties by electron microscopy. These antibody studies have provided defined landmarks as well as procedures for the separation of different forms of NCAM. As a result, it has been possible not only to observe the molecule by electron microscopy, but also to relate its shape to known chemical and biological properties.

Materials and Methods

Purification of NCAM

Membranes were prepared from embryonic day 14 (E14) chicken brains as described (11, 14). Membrane material was mixed with 15 times pellet volume in PBS plus 0.5% NP-40 for 30 min at 4°C, and separated by centrifugation at 35,000 rpm for 15 min (Ti60 rotor; Beckman Instruments, Inc., Palo Alto, CA). Soluble material was first applied to a Sepharose 4B column coupled (3) with monoclonal antibody PP prepared against chicken NCAM (26), which recognizes an extracellular portion of the NCAM polypeptide that is shared by the 160-, 130- and 110-kD forms (30). Bound proteins were eluted with diethylamine buffer (14), neutralized, and applied to a second Sepharose 4B column coupled with NCAM monoclonal antibody 4D. Antibody 4D reacts with an intracellular epitope present only on the 160-kD NCAM polypeptide (30). The unbound 130-kD rich NCAM fraction was collected, and the bound 160-kD rich NCAM eluted. NCAM preparations were dialyzed extensively against PBS.

Polypeptide Composition of NCAM Preparations

Both preparations of NCAM were free of non-NCAM proteins as judged

© The Rockefeller University Press, 0021-9525/87/06/1579/8 $1.00

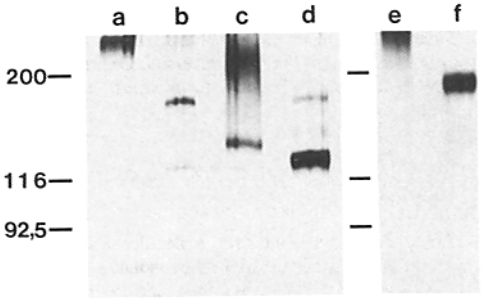

Figure 1. SDS PAGE analysis of immunoaffinity-purified NCAM, before and after treatment with endo F to remove N-linked carbohydrates. (Lane *a*) 160-kD rich NCAM that bound to antibody 4D-Sepharose beads; (lane *b*) 160-kD rich NCAM after endo F treatment; (lane *c*) 130-kD rich NCAM that did not bind to 4D-conjugated Sepharose; (lane *d*) 130-kD rich NCAM after endo F treatment. Also shown are the 160-kD rich NCAM preparation before (lane *e*) and after (lane *f*) treatment with endo N to remove polysialic acid. Molecular mass standards indicated by kilodaltons refer to myosin, beta-galactosidase, and phosphorylase b. Proteins are visualized by silver staining (19).

by SDS PAGE (15). Electrophoresis was carried out as described using 8 × 6-cm gels of 7.5% acrylamide with stacking gels of 3% acrylamide.

The soluble endoglycosidase from F. meningosepticum (endo F) (provided by Dr. J. Elder and Dr. S. Alexander, Scripps Clinic and Research Foundation, La Jolla, CA; reference 7) was used to remove N-linked carbohydrates from NCAM. Samples were mixed 1:1 with pH 6.1 buffer containing 100 mM sodium phosphate, 50 mM EDTA, 1% NP-40, 1% mercaptoethanol, and 0.1% SDS, and boiled for 2 min at 100°C to denature the molecule. Samples were then mixed with endo F in glycerol at a final ratio of 1 U enzyme per 2 μg protein, and incubated at 37°C for 2 h. SDS PAGE sample buffer was added, and samples were heated for 3 min at 100°C before application to the gel.

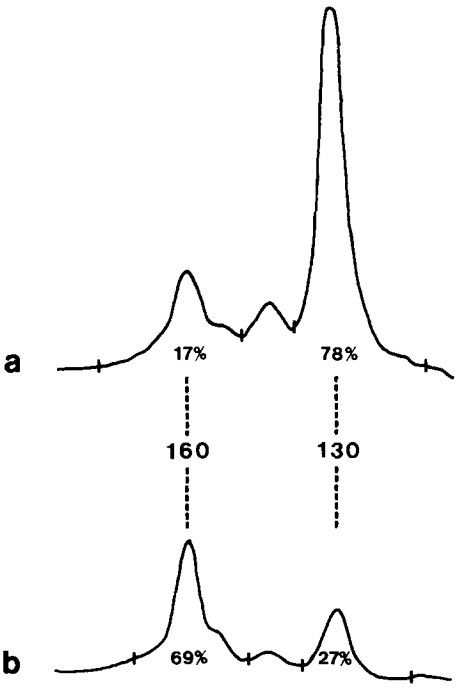

Figure 2. Composition of NCAM preparations as determined by densitometric analysis of silver-stained gels. Deglycosylated NCAM forms in Fig. 1, lanes *b* and *d* were scanned to quantify the relative amounts of the 160- and 130-kD NCAM polypeptides in each preparation. The percentage of the total absorbance is indicated for each peak. (*a*) Endo F–treated 130-kD rich NCAM; (*b*) endo F–treated 160-kD rich NCAM.

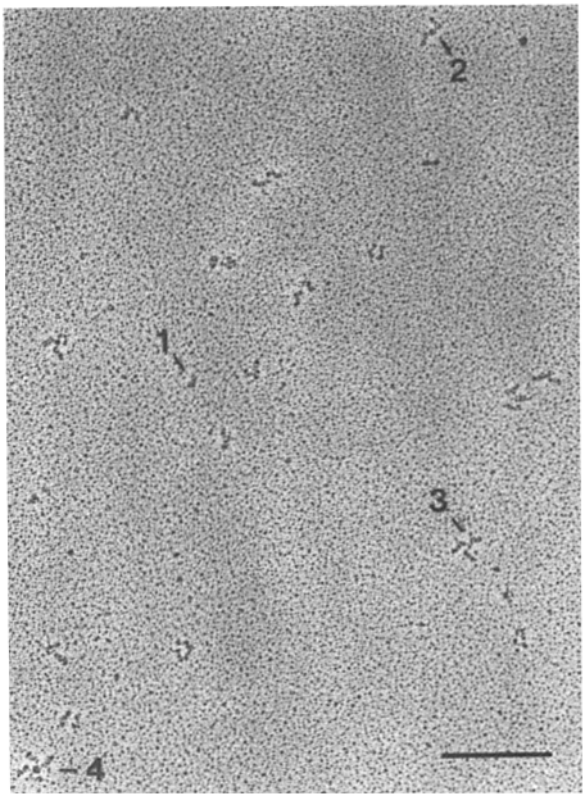

Figure 3. Field of rotary-shadowed NCAM molecules with a variety of pinwheel forms. Examples of single and multi-arm aggregates are indicated. Bar, 200 nm.

Removal of the polysialic acid from NCAM was performed with purified phage endoneuraminidase (endo N; reference 29) that specifically cleaves long chain alpha 2,8 polysialic acids (gift of Dr. E. R. Vimr, University of Illinois, Urbana-Champaign, IL). For thorough digestion, endo-N was mixed with NCAM at 2 U/μg NCAM, and incubated for 8 h at 37°C.

Silver staining of proteins separated by gel electrophoresis was performed according to (19) and the silver stained gels were analyzed with a gel scanner at 575-nm wavelength (model CS-930; Shimadzu Scientific Instruments, Inc., Columbia, MD).

Low Angle Rotary Shadowing and Frozen Replication of NCAM

Molecular shadowing of purified NCAM molecules was performed by standard methods (27, 25, 13) with the following modifications. Protein solutions diluted to 50 μg/ml in 50–500 mM ammonium acetate (pH 6.8) were mixed with 2 vol of glycerol and sprayed onto mica using a JetPak sprayer (Sprayon Products, Bedford Heights, OH). For antibody-NCAM preparations, antibody (20–50 μg/ml) and NCAM (100 μg/ml) were mixed in 10 mM imidazole, 50 mM KCl buffer, pH 7.2 (reference 10), or 50 mM ammonium acetate (pH 6.8) and incubated either at 23°C for 2–6 h or overnight at 4°C before mixing with glycerol and spraying. Mica samples were placed in a freeze-etch machine (model 360; Balzers, Hudson, NH) equipped with a rotary stage and evacuated to 2×10^{-6} torr for at least 5 min at room temperature, shadowed at 5 degrees with a platinum/tantalum/iridium mixture (16), and coated with a supporting film of carbon. To examine NCAM under hydrated conditions, mica chip frozen replication was carried out as described (13) using NCAM (100 μg/ml) applied to the mica slurry on a gelatin support. Replicas were collected on clean 400 Hex copper grids, and examined at 120 KeV in a JEOL 200 CX electron microscope equipped with a multimeter (model 901; Keithley Instruments, Inc., Cleveland, OH) to measure lens current, as an index of magnification. Actual magnification was determined by calibration with carbon line grids (Polysciences, Inc., Warrington, PA). Z axes were adjusted so micrographs were taken at 68,750×.

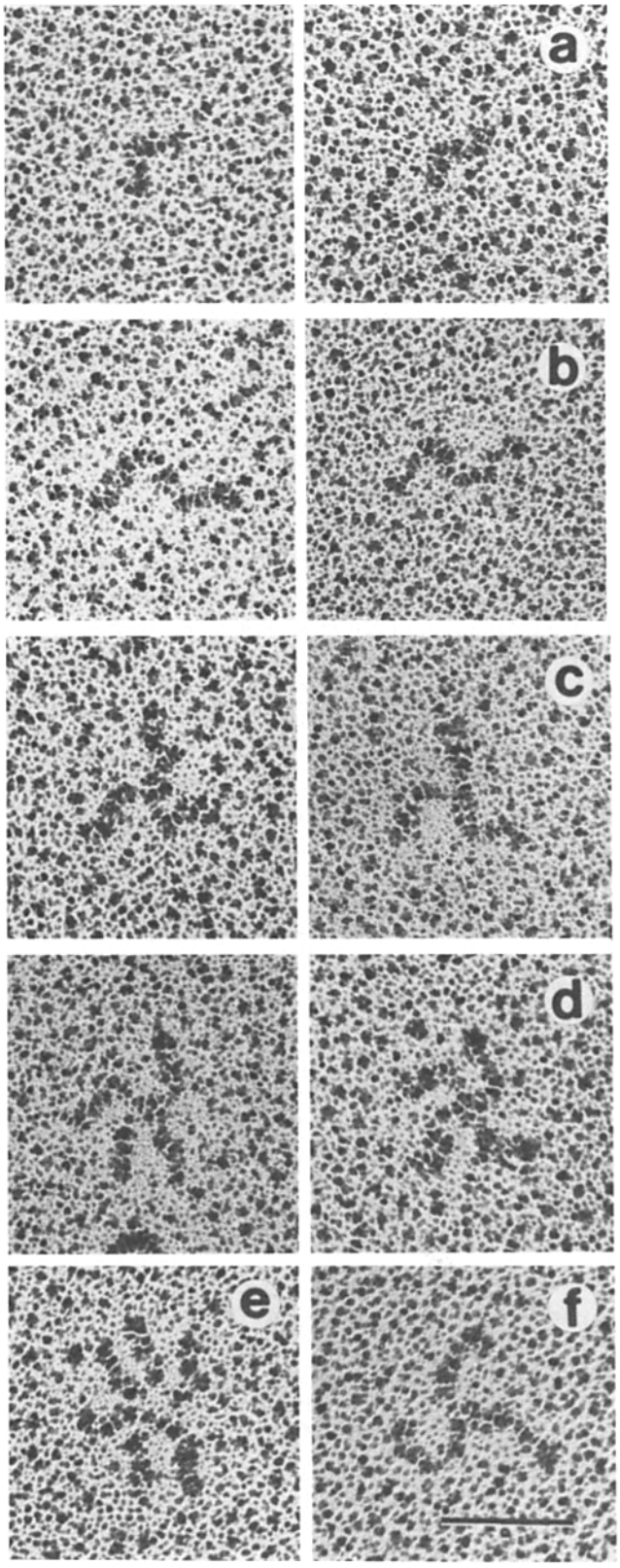

Figure 4. Selected rotary-shadowed 160-kD rich NCAM pinwheel figures with (*a*) one, (*b*) two, (*c*) three, (*d*) four, and (*e*) six arms; (*f*) clathrin triskelion. Bar, 50 nm.

Micrograph negatives were cut to 35-mm widths and inserted into a motion analyser (Vanguard, Melville, NY) to digitize molecular measurements directly from the negative. The final magnification at which measurements were made was 838, 750×.

Shadow thickness was estimated from increases in the known sizes of myosin (gift of Dr. M. Sheetz, Washington University, St. Louis, MO) and clathrin (obtained from Dr. D. Shotton, Oxford University, Oxford, United Kingdom) added to the NCAM proteins. The shadow thickness varied from 2–3 nm.

Measurement of Molecular Lengths and Analysis of Populations

All studies were based on photographs of fields of molecules selected only for shadow quality and freedom from salt crystals. Only isolated, extended, and clearly visible molecules were used for analyses, and the number of molecules not fitting these criteria was noted (~1% of the total figures). To determine the length of NCAM molecules, single rods or pinwheel arms were measured from the first to the last visible metal grain, or from the pinwheel center to the last metal grain, through the longitudinal center of the arm. The width of the arms was measured through the middle of a segment, including first and last distinguishable metal grains.

Results

Characterization of Different NCAM Preparations

NCAM was isolated by affinity chromatography from detergent extracts of brain membranes using a monoclonal antibody (PP) directed against an extracellular epitope associated with both the 160- and 130-kD polypeptide forms of NCAM (30). This mixture of NCAM polypeptides was further fractionated by affinity chromatography using a second monoclonal antibody (4D) which recognizes an epitope present on the longer 160-kD NCAM, but absent on the shorter 130-kD NCAM form (30). In this manner, two populations enriched in either 160- or 130-kD NCAM were prepared. Although NCAM is also produced in a 110-kD form, apparently by glial cells that appear in older embryos (18), this polypeptide was not detected in the present preparations obtained from E14 chick embryos.

To assess the composition of these preparations, the large amount of N-linked carbohydrate associated with E14 chicken NCAM, which alters the mobility of NCAM polypeptides on reducing SDS PAGE gels, was enzymatically removed using endo F (Fig. 1, reference 7). After endo F treatment, NCAM appeared as sharp bands with molecular masses of 160- and 130-kD. The relative amounts of NCAM polypeptides in the two preparations were then quantified by densitometry (Fig. 2). These results indicated that the 130-kD enriched NCAM consisted of ~80% 130-kD and 20% 160-kD forms, whereas the 160-kD enriched NCAM contained ~30% 130-kD and 70% 160-kD forms. These two enriched populations were used for all further studies, with the full complement of carbohydrates attached unless noted.

General Appearance of NCAM in Electron Micrographs

Both NCAM preparations contained structures with similar morphological features, most notably single bent rods of uniform thickness which often appeared as pinwheel-like aggregates (Figs. 3 and 4). The bent arms of most aggregates were typically oriented in the same direction about the molecule, and were evenly spaced from one another, suggesting that interactions are restricted to particular associations.

1. *Abbreviations used in this paper*: Endo F, the soluble endoglycosidase from F. meningosepticum; endo N, the soluble endoneuraminidase from KlF bacteriophage; NCAM, neural cell adhesion molecule.

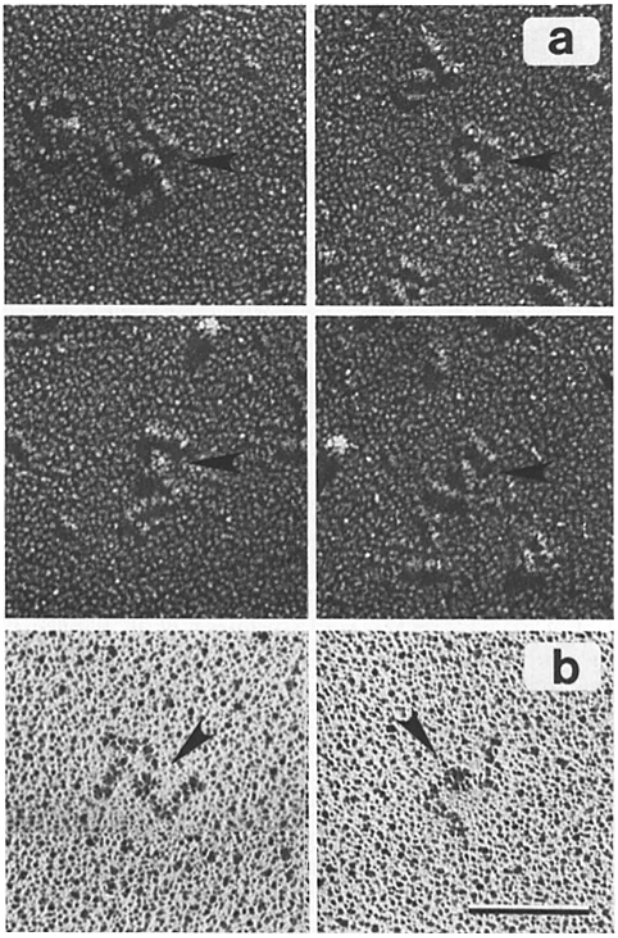

Figure 5. Large globular regions near the center of the pinwheel found associated with half of NCAM figures observed. (*a*) NCAM-160 as visualized by frozen replication. (*b*) Selected low angle rotary shadow images of NCAM-160 with pronounced central globules. Bar, 50 nm.

Most of the rods were similar in size except for occasional smaller pieces which may represent NCAM fragments produced by shearing or proteolysis.

The rod-shaped arms of the NCAM figures had a relatively even thickness (7–8 nm) along their length. Metal shadow

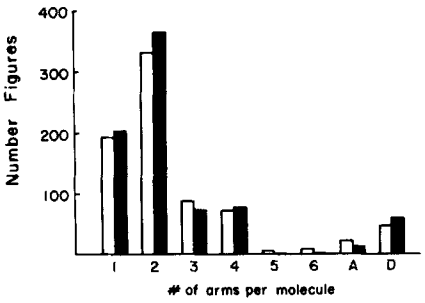

Figure 6. Frequency histogram of the number of molecular figures present as single rods and as multi-arm pinwheels in the 130-kD (*open bars*) and 160-kD (*shaded bars*) rich NCAM preparations. Aggregates of greater than six arms (*A*) and discarded molecules (*D*) whose arm number could not be determined are indicated, but were not used in subsequent statistical analyses.

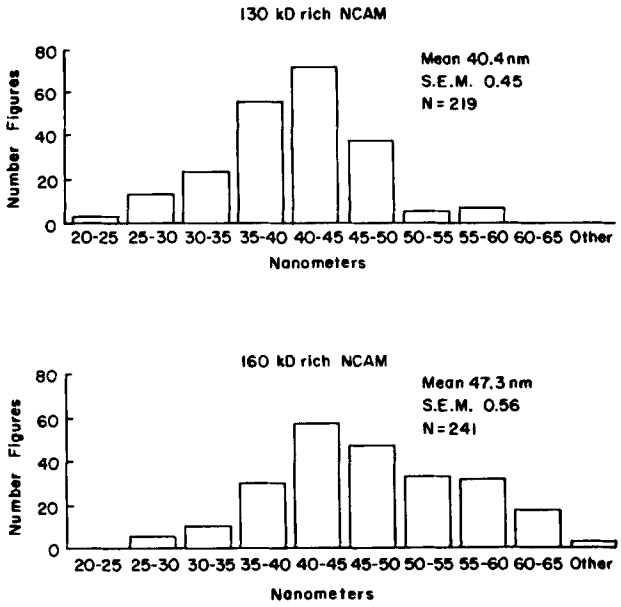

Figure 7. Frequency histograms of arm lengths in the 130- and 160-kD rich NCAM preparations. The mean length of each pool is indicated.

thickness in most preparations was 2–3 nm, so that the actual thickness of an NCAM arm is estimated to be 4–5 nm. The uniformity in thickness is reflected in the observation that the ratio of molecular masses (130:160 = 0.81) is similar to the ratio of adjusted mean lengths (38:51 nm = 0.75; see below).

The angle of the bend varied considerably, but usually ranged from 90 to 110 degrees. This variability suggests that the molecule is flexible at the bend. Another nonlinear region was seen near the periphery of ~30% of the arms in both the 130- and 160-kD rich NCAM samples (see Fig. 4 *c*, right). This feature was not associated with additional arm length, and therefore could also represent a flexible region of the molecule.

Approximately half of the multi-arm structures seen contained additional globular material at the hub of the pinwheel (Fig. 5). Frozen replication of NCAM-160 (Fig. 5 *a*) produced figures similar to those seen with low angle rotary shadowing, except that the central globule was more frequently observed. Frozen replication of a molecule has the advantage not only of preserving hydrated structures, but also allows molecules to orient on the negatively charged mica surface in an aqueous buffer. Therefore, the globular regions may reflect a particular orientation of the NCAM molecules or additional charged material at the center of the pinwheel.

Aggregation State of NCAM

30% of NCAM figures appeared as single rods, 50% as doubles, and aggregates with three and four arms each composed 7–10% of each population (Fig. 6). No difference between the 130- and 160-kD rich NCAM pools was detected in the prevalence of particular aggregated states (Chi square test, 5 DF, 0.95).

To minimize nonspecific hydrophobic interactions between the membrane-spanning regions of NCAM molecules, all experiments shown were carried out in the presence of detergent. Attempts were also made to disrupt the aggregated

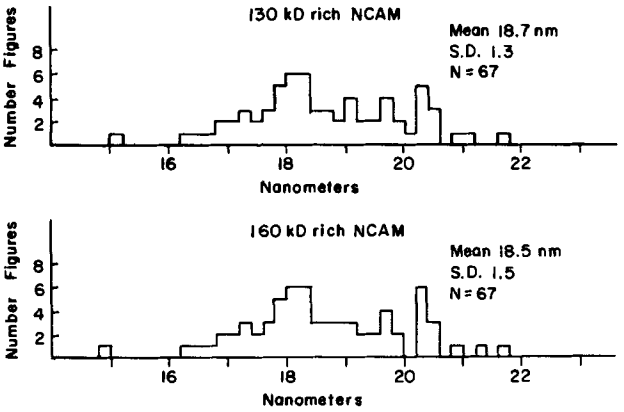

Figure 8. Frequency histograms of the measured distance between the center of the pinwheel to the bend in each arm for the 130- and 160-kD rich NCAM preparations. The broad distribution of arm lengths for these populations is due in part to the 130 contamination of the 160 NCAM preparations (and vice versa) but also reflects differences in the orientation of molecules on the mica surface. When compared, no difference in this measurement was seen between the 130- and 160-kD rich NCAM (paired t test, $n = 67$, $P < 0.001$).

molecules by alterations in pH or salt concentration. The treatments (30 min at 25°C before mixing with glycerol) included 2 M potassium iodide, 100 mM NaOH, 1% deoxycholate, 2% SDS, or 4 M guanidine HCl. However, none of these treatments altered the observed state of aggregation of NCAM molecules (data not shown).

Length of NCAM Arms

Measurements of arm lengths in 460 molecules were plotted in histogram form (Fig. 7) and their distribution subjected to statistical analysis. The mean length of arms in the 130-kD rich NCAM preparation was 40.4 nm (SEM 0.45 nm, $n = 219$), while the 160-kD rich preparation had arms with a mean length of 47.3 nm (SEM 0.56 nm, $n = 241$). To correct for the presence of cross-contamination in the two NCAM preparations, these mean lengths were adjusted by the percentage contamination with the minor component. This correction gave estimated lengths of 38 nm for the 130-kD NCAM and 51 nm for 160-kD NCAM. In pinwheel structures found in both preparations, the bend or hinge region of each arm reproducibly occurred 18.5 nm from the central pinwheel hub (Fig. 8). Thus, the difference in length between the 130- and 160-kD molecules was associated with the peripheral part of each arm, distal to the bend.

Effects of Polysialic Acid Removal

The polysialic acid moieties of NCAM can be selectively cleaved using endo N (29), a treatment that enhances cell-cell adhesion mediated by the molecule (24). To examine the effect of polysialic acid removal on aggregation of isolated NCAM molecules, the 160-kD enriched population was treated with endo N. The extent of polysialic acid removal obtained with endo N was monitored by gel electrophoresis (Fig. 1, lanes *e* and *f*). This treatment removes most of the NCAM carbohydrate, but leaves several short (3–6 kD, reference 7) carbohydrate units. Random fields of endo N–treated NCAM were then analyzed for the number of arms per molecule, and the frequencies of each aggregate were compared

Table I. Effect of Endo N Treatment on NCAM Aggregation

No. arms	Control	Treated	Change
	%	%	%
1	29.3	14.5	−14.8
2	50.6	57.6	+7.0
3	13.1	22.1	+9.0
4	7.0	5.8	−1.2

Numbers indicate the frequency of a particular aggregated state in random samples of the 160-kD enriched NCAM preparation. 172 figures were counted in the endo N–treated group and 670 figures were in the control group. The percentage of large aggregates or indistinct figures was the same (1%) for both groups.

with the untreated control (Table I). After endo N treatment, no difference was seen in the appearance of individual NCAM molecules, consistent with previous reports that carbohydrate moieties are difficult to visualize by rotary shadowing techniques (25). However, endo N–treated NCAM was significantly more aggregated than the control NCAM (Chi square test, 4 DF, 0.95), with a decrease in the number of single arms and a concomitant increase in the number of two- and three-arm aggregates.

Localization of Monoclonal Antibody Epitopes

Due to their Y-shaped structure, rotary shadowed immunoglobulin molecules often have a distinctive triangular appearance in electron micrographs, which aids in their identification. These antibody figures are relatively large, thereby limiting the absolute resolution of electron microscopic epitope mapping to ~15 nm. Four monoclonal antibodies that react with defined sites on the NCAM polypeptide were used to identify key features on the observed molecular structures. Well-formed pinwheel aggregates of NCAM were chosen for examination to aid in the orientation of arms. To minimize nonspecific binding of antibodies to the molecule, it was necessary to titrate the amount of each antibody used and to vary the incubations (Fig. 9). Control nonimmune immunoglobulin was only infrequently associated with NCAM pinwheels, and in these cases was distributed randomly over the figures (data not shown). Antibodies 30B and 4D, which recognize different intracellular epitopes found only on the 160-kD NCAM, bound specifically to the distal tips of the pinwheel arms. Antibody 5E, whose epitope has been localized near the heparin–NCAM binding site (8) and which is within 25 kD of the NCAM NH_2-terminus, bound near the center of the pinwheel figures. Epitope 105, which was present near the middle of the 160-kD polypeptide and the site of polysialic acid attachment, was observed near the hinge region (Table II). When 30B and 5E together were incubated with NCAM, about one-quarter of the antibody-labeled figures had antibodies at both the center and distal tip (Fig. 9 *e*).

Discussion

To examine the shape and aggregation state of the NCAM molecule, electron micrographs of NCAM preparations have been used to compare the 160- and 130-kD forms of the molecule as well as those having different amounts of polysialic acid. In addition, monoclonal antibody epitopes associated with known regions of the polypeptide chain have been local-

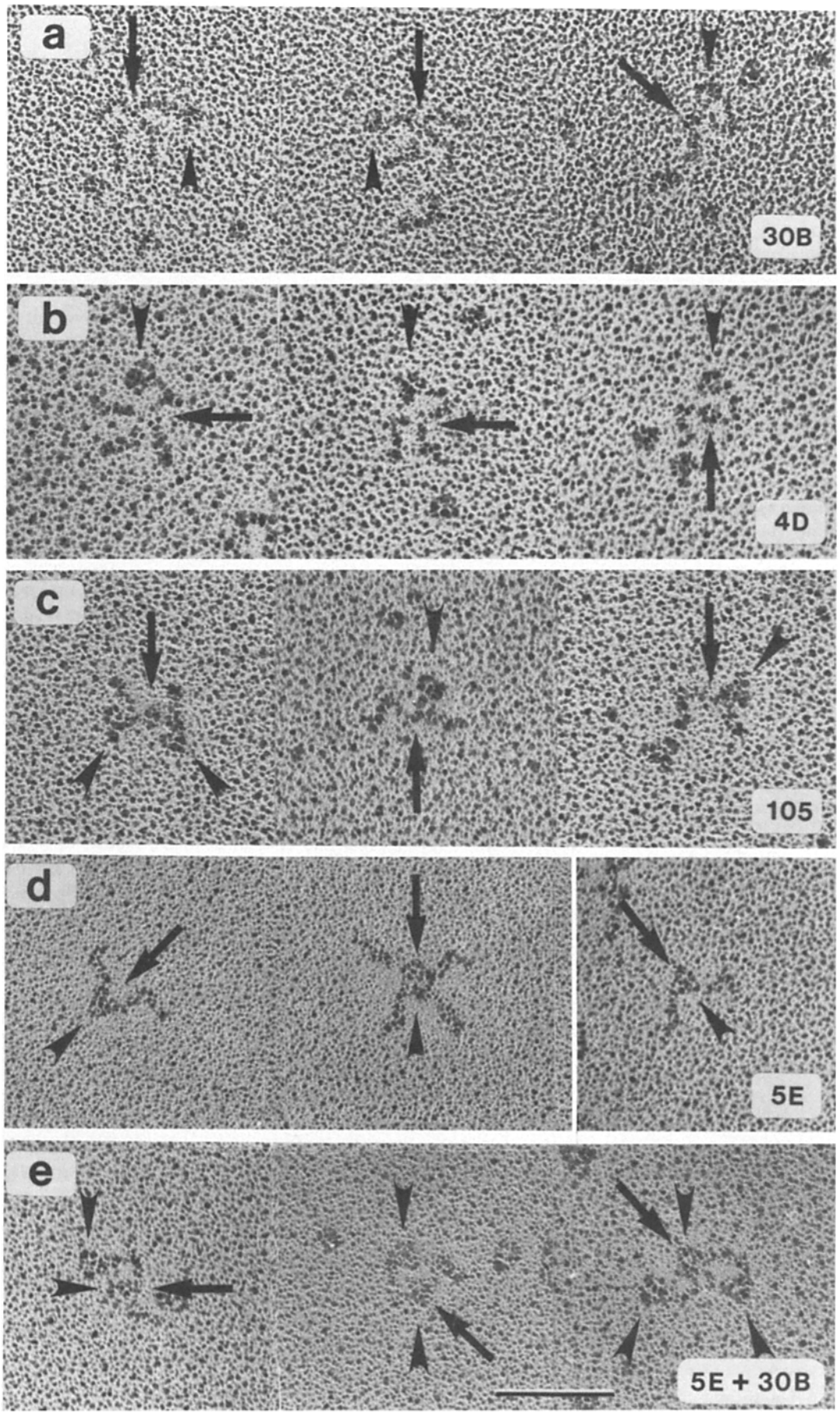
a
30B
b
4D
c
105
d
5E
e
5E + 30B

Table II. Localization of Monoclonal Antibody Epitopes

Antibody	No. of figures	Total No. of arms	Arms with bound antibody	Epitope location on pinwheel		
				Center	bend	tip
30B	57	144	37	5	0	32
4D	22	67	15	0	0	15
105	92	179	36	4	30	2
5E	52	114	40	31	0	9

Electron micrographs were scored for the presence of triangular antibody molecules in close apposition to NCAM figures. Center, the region from the pinwheel hub up to the bend; bend, the region from the arm bend to the middle of the distal segment; tip, includes antibodies bound from the middle to the tip of the distal segment.

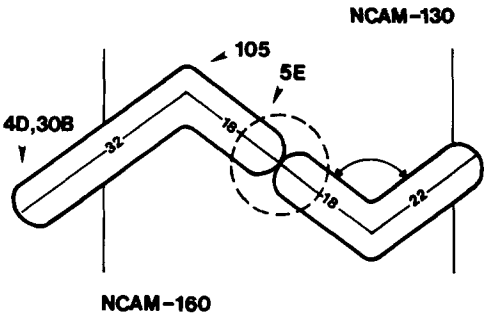

Figure 10. A schematic model of a 130/160-kD heterodimer of NCAM. Approximate location of each monoclonal antibody is indicated by arrows. The globular structure found in about one-half of NCAM figures is indicated near the center. The inferred placement of the plasma membrane is drawn behind the heterodimer. Molecular lengths are indicated in nanometers.

ized on the molecular images. The combined results have led to several predictions (Fig. 10) about the molecular nature of NCAM-mediated cell–cell bonds.

Our interpretation of NCAM figures in electron micrographs is dependent on the description of NCAM monomers as bent rods either 40 or 50 nm in length and with a diameter of 4–5 nm. One-third of the figures in the NCAM samples were in fact single bent rods of these dimensions. Furthermore, the arms in the pinwheel figures matched this description. An alternative model, with two monomers lying side by side to form a single arm, is unlikely in the absence of "split" arms. Another possibility, that the monomer spans the length of two pinwheel arms, is difficult to reconcile with the similarity in the overall dimensions of NCAM and the 180-kD clathrin subunit (45 nm; see Fig. 4 *f*, and reference 28), as well as the presence of figures with an odd number of arms. Finally, while single arms seldom exhibited multiple sites for a particular monoclonal antibody, pinwheel aggregates did bind the same antibody to each of several arms, supporting the argument that each arm represents a complete NCAM monomer.

This description of an NCAM monomer and its ability to aggregate in solution is consistent with previous studies on the properties of the purified molecule. Hoffman et al. (14) found that NCAM preparations are polydisperse in solution, with gel filtration molecular masses ranging from 0.5 to 1.2 $\times$ 10^6 D. Therefore, assuming a monomeric molecular mass of 200–250 kD for the glycosylated molecule, NCAM appears to exist in solution as aggregates of approximately two to six molecules (14). In electron micrographs, a similar range of aggregates was observed, with dimers as the most prevalent multimeric form. Preliminary reports on the appearance of purified NCAM in electron micrographs (5, 6) suggested that tripartate structures analogous to clathrin were the predominant form. However, in the present study, although the higher aggregates were seen and had a regular structure, monomers and dimers accounted for 80% of NCAM figures and three-arm structures represented only 10% of the population. While the aggregates of purified NCAM demonstrated by electron microscopy may not be representative of the molecule's binding behavior in the cell membrane, they are consistent with the functional description of NCAM as a homophilic ligand mediating cell–cell binding (23). Whereas the observed dimers could represent a simple end to end joining of two molecules (Fig. 10), the less frequently occurring higher order aggregates may reflect a stacking of such dimers, or the addition of monomers to form a ring-like structure at the pinwheel hub.

The present studies provide several reasons to believe that NCAM aggregates in solution are related to the molecule's activity in the cell membrane. First, the length difference in the distal portion of the pinwheel arms between the 130- and 160-kD NCAM forms corresponds to the known cytoplasmic length heterogeneity between these polypeptides, indicating that the segments of uniform length that interact in the center of the pinwheel represent the extracellular portion of the molecule. Second, the locations of monoclonal antibody epitopes indicate that the observed NCAM rod aggregation involves contact between the region of the molecule believed to participate in cell–cell binding. Finally, the enzymatic removal of the NCAM polysialic acid domain, which has been shown to increase the rate of NCAM-mediated aggregation of membrane vesicles (24) also enhanced the degree of aggregation among isolated NCAM molecules.

Half of the pinwheel aggregates had, in addition to NCAM arms, a globular structure at the central hub. It is therefore possible that a variable feature or second molecule is associated with NCAM near its binding site. The central hub was more prevalent in frozen hydrated preparations than in dehydrated samples. One possibility for a hydration-sensitive or charged structure would be a large carbohydrate, such as the polysialic acid component of NCAM. Though the attachment site of the polysialic acid–rich carbohydrate of NCAM is thought to be located in the middle of the molecule (2), the bulk of the carbohydrate could extend toward the binding region. Alternatively, it has been proposed that a heparin-like molecule binds to the NH_2-terminal region of NCAM

Figure 9. Monoclonal antibodies bound to distinct regions on NCAM pinwheel figures. The center of each aggregate is indicated with an arrow, and antibodies are shown with arrowheads. (*a*) Antibody 30B bound to the distal region of one arm on each of two tetramers, and to one arm of a dimer. (*b*) Antibody 4D bound to the distal region of one arm of a tetramer, trimer, and dimer. (*c*) Antibody 105 bound near the arm bend of three dimers. (*d*) Antibody 5E bound near the pinwheel center of a dimer, tetramer, and dimer. (*e*) 5E and 30B doubly labeled dimers, with antibody at both the pinwheel center, and distal region. Bar, 50 nm.

(8) and may act to augment homophilic NCAM-mediated adhesion (1). Thus, another candidate would be a heparan sulfate proteoglycan, which is of the appropriate size (17) and which could have copurified with NCAM during affinity isolation. However, similar preparations of NCAM used in earlier studies did not appear to contain substantial amounts of uronic acids (14).

At the cellular level, an important question remains as to whether the molecular dimensions obtained by electron microscopy are consistent with the membrane–membrane distances observed between cells that are bound together by an NCAM-dependent adhesion mechanism. A typical distance between plasma membranes in an aggregate of embryonic chick retinal cells is <30 nm (our unpublished observations). Assuming a constant diameter along an NCAM arm, the known molecular mass of the extracellular domain (108 kD) would correspond to a length of 34 nm. It follows, therefore, that two NCAM molecules, bound end to end and oriented away from their respective plasma membranes, must have sufficient internal flexibility to fit within the observed cell–cell distance (Fig. 10). The flexible hinge that exists within each NCAM monomer could provide for this adjustment, and allow the bond to span a considerable range of intercellular spacings.

The authors thank Tom Reese for his support and discussion of this work, Larry Frelinger for initial preparation of NCAM samples, and Ann Acheson for review of the manuscript.

This work was supported in part by National Institutes of Health grants HD-18369 and EY-06107. A. K. Hall is supported by U.S. Public Health Service training grant HD-07104.

Received for publication 24 September 1986, and in revised form 23 February 1987.

References

1. Cole, G. J., A. Loewy, and L. Glaser. 1986. Neuronal cell-cell adhesion depends on interactions of NCAM with heparin-like molecules. *Nature (Lond.).* 320:445–447.
2. Crossin, K. L., G. M. Edelman, and B. A. Cunningham. 1984. Mapping of three carbohydrate attachment sites in embryonic and adult forms of the neural cell adhesion molecule. *J. Cell Biol.* 99:1848–1855.
3. Cuatrecasas, P., and C. B. Anfinsen. 1971. Affinity chromatography. *Methods Enzymol.* 22:345–378.
4. Cunningham, B. A., S. Hoffman, U. Rutishauser, J. J. Hemperly, and G. M. Edelman. 1983. Molecular topography of the neural cell adhesion molecule NCAM: surface orientation and location of sialic-acid rich and binding regions. *Proc. Natl. Acad. Sci. USA.* 80:3116–3120.
5. Edelman, G. M. 1984. Modulation of cell adhesion during induction, histogenesis, and perinatal development of the nervous system. *Annu. Rev. Neurosci.* 7:339–377.
6. Edelman, G. M., S. Hoffman, C.-M. Chuong, J.-P. Thiery, R. Brackenbury, W. J. Gallin, M. Grumet, M. E. Greenberg, J. J. Hemperly, C. Cohen, and B. A. Cunningham. 1983. Structure and modulation of neural cell adhesion molecules in early and late embryogenesis. *Cold Spring Harbor Symp. Quant. Biol.* 48:515–526.
7. Elder, J. H., and S. Alexander. 1982. Endo B-N acetylglucosaminidase F: endoglycosidase from Flavobacterium meningosepticum that cleaves both high mannose and complex glycoproteins. *Proc. Natl. Acad. Sci.* 79:4540–4544.
8. Frelinger, A. L., and U. Rutishauser. 1986. Topology of NCAM structural and functional determinants. II. Placement of monoclonal antibody epitopes. *J. Cell Biol.* 103:1729–1737.
9. Gennarini, G., M. Hirn, H. Deagostini-Bazin, and C. Goridis. 1984. Studies on the transmembrane disposition of the neural cell adhesion molecule N-CAM. The use of liposome-inserted radioiodinated N-CAM to study its transbilayer orientation. *Eur. J. Biochem.* 142:65–73.
10. Glenney, J. R., P. Glenney, and K. Weber. 1983. Mapping the fodrin molecule with monoclonal antibodies. A general approach for rod-like multidomain proteins. *J. Mol. Biol.* 167:275–293.
11. Hall, A. K., and U. Rutishauser. 1985. Phylogeny of a neural cell adhesion molecule. *Dev. Biol.* 110:39–46.
12. Hemperly, J. J., B. A. Murray, G. M. Edelman, and B. A. Cunningham. 1986. Sequence of a cDNA clone encoding the polysialic acid-rich and cytoplasmic domains of the neural cell adhesion molecule N-CAM. *Proc. Natl. Acad. Sci. USA.* 83:3037–3041.
13. Heuser, J. E. 1983. Procedure for freeze drying molecules adsorbed to mica flakes. *J. Mol. Biol.* 169:155–195.
14. Hoffman, S., B. C. Sorkin, P. C. White, R. Brackenbury, R. Mailhammer, U. Rutishauser, B. A. Cunningham, and G. M. Edelman. 1982. Chemical characterization of a neural cell adhesion molecule purified from embryonic brain membrane. *J. Biol. Chem.* 257:7720–7729.
15. Laemmli, U. K. 1970. Cleavage of structural protein during assembly of the head of bacteriophage T4. *Nature (Lond.).* 227:680–685.
16. Landis, D. M. D., T. S. Reese, R. L. Ornberg, and W. F. Graham. 1981. Substructure of astrocytic assemblies. *Soc. Neurosci. Abstr.* 7:305.
17. Laurie, G. W., J. T. Bing, H. K. Kleinman, J. R. Hassell, M. Aumailley, G. R. Martin, and R. J. Feldmann. 1986. Localization of binding sites for laminin, heparan sulfate proteoglycan and fibronectin on basement membrane (type IV) collagen. *J. Mol. Biol.* 189:205–216.
18. Noble, M., F. M. Albrechtsen, C. Moller, J. Lyles, E. Bock, C. Goridis, M. Watanabe, and U. Rutishauser. 1985. Glial cells express NCAM/D2-CAM-like molecules in vitro. *Nature (Lond.).* 316:725–728.
19. Oakley, B. R., D. R. Kirsh, and N. R. Morris. 1980. A simplified ultrasensitive silver stain for detecting proteins in polyacrylamide gels. *Anal. Biochem.* 105:361–363.
20. Rougon, G., and D. R. Marshak. 1986. Structural and immunological characterization of the amino-terminal domain of mammalian neural cell adhesion molecule. *J. Biol. Chem.* 261:3396–3401.
21. Rutishauser, U. 1984. Developmental biology of a neural cell adhesion molecule. *Nature (Lond.).* 310:549–554.
22. Rutishauser, U., and C. Goridis. 1986. NCAM: the molecule and its genetics. *Trends Genet.* 2:72–76.
23. Rutishauser, U., S. Hoffman, and G. M. Edelman. 1982. Binding properties of a cell adhesion molecule from neural tissue. *Proc. Natl. Acad. Sci. USA.* 79:685–689.
24. Rutishauser, U., M. Watanabe, J. Silver, F. A. Troy, and E. R. Vimr. 1985. Specific alteration of NCAM-mediated cell adhesion by an endoneuraminidase. *J. Cell Biol.* 101:1842–1849.
25. Slayter, H. S. 1976. High-resolution metal replication of macromolecules. *Ultramicroscopy.* 1:341–357.
26. Thanos, S., F. Bonhoeffer, and U. Rutishauser. 1984. Fiber-fiber interactions and tectal cues influence the development of the chick retiontectal projection. *Proc. Natl. Acad. Sci. USA.* 81:1906–1910.
27. Tyler, J. M., and D. Branton. 1980. Rotary shadowing of extended molecules dried from glycerol. *J. Ultrastr. Res.* 71:95–102.
28. Ungewickell, E., and D. Branton. 1981. Assembly units of clathrin coats. *Nature (Lond.).* 289:420–422.
29. Vimr, E. R., R. D. McCoy, H. F. Vollger, N. C. Wilkinson, and F. A. Troy. 1984. Use of prokaryotic-derived probes to identify poly (sialic acid) in neonatal membranes. *Proc. Natl. Acad. Sci. USA.* 81:1971–1975.
30. Watanabe, M., A. L. Frelinger, and U. Rutishauser. 1986. Topology of NCAM structural and functional determinants. I. Classification of monoclonal antibody epitopes. *J. Cell Biol.* 103:1721–1727.